Research Article/Mechanical Engineering, Mechatronics, and Materials Science http://doi.org/10.15446/ing.investig.107624

Influence of Thermal Aging on the Sliding Wear of a Biocomposite Material Reinforced with Bamboo Fibers

Influencia del envejecimiento térmico sobre el desgaste deslizante de un material biocompuesto reforzado con fibras de bambú

Eudi Blanco[1], Jorge I. Fajardo[2], Edwuin J. Carrasquero[3], Caribay Urbina[4], Luis M. López[5], and Luis Cruz[6]

ABSTRACT

This study evaluated the effect of thermal aging on the tribological properties of biocomposites formed by an isotactic polypropylene matrix (iPP) reinforced with 20 wt% (PP/20F), 30 wt% (PP/30F), and 40 wt% (PP/40F) of randomly oriented bamboo fibers. iPP, along with the grafting of maleic anhydride molecules (MAPP), was used as a coupling agent. The accelerated thermal aging involved the continuous heating of the materials at 98 ˚C for 10 days. Wear tests were performed under the Pin-on-Disk configuration to determine the wear factor (K) and the friction coefficient (μ) of the materials. After thermal aging, the μ value of the PP/20F composite increased by 40.5%, while, for raw PP, PP/30F, and PP/40F, the increase was 2.1, 7.5, and 2.2%, respectively. The aged PP/30F composite achieved the highest μ value. The loss of wear resistance due to aging was more prominent in the raw PP. The K factor of the aged and unaged PP/20F was the lowest. The use of scanning electron microscopy allowed identifying that adhesive, abrasive, and fatigue wear mechanisms were the dominant ones.

Keywords: polypropylene, natural fiber, bamboo, biocomposite, tribology, sliding wear, wear rate, coefficient of friction, aging

RESUMEN

En este estudio se evaluó el efecto del envejecimiento térmico sobre las propiedades tribológicas de biocompuestos formados por una matriz de polipropileno isotáctico (iPP) reforzada con 20 wt% (PP/20F), 30 wt% (PP/30F) y 40 wt% (PP/40F) de fibras de bambú orientadas al azar. Se utilizó iPP con injertos de moléculas de anhídrido maleico (MAPP) como agente de acople. El envejecimiento térmico acelerado consistió en un calentamiento continuo de los materiales a 98 ˚C durante 10 días. Se realizaron ensayos de desgaste bajo la configuración *Pin-on-Disk* para determinar el factor de desgaste (K) y el coeficiente de fricción (μ) de los materiales. Después del envejecimiento térmico, el valor de μ del compuesto PP/20F aumentó en un 40.5 %, mientras que, para el PP puro, PP/30F y PP/40F, el aumento fue de 2.1, 7.5 y 2.2 % respectivamente. El compuesto PP/30F envejecido alcanzó el mayor valor de μ. La pérdida de la resistencia al desgaste debido al envejecimiento fue más resaltante en el PP puro. El factor K del PP/20F envejecido y no envejecido fue el más bajo. El uso de microscopía electrónica de barrido permitió identificar que los mecanismos de desgaste adhesivo, abrasivo y por fatiga fueron los dominantes.

Palabras clave: polipropileno, fibra natural, bambú, biocompuesto, tribología, desgaste deslizante, tasa de desgaste, coeficiente de fricción, envejecimiento

Received: March 4th, 2023
Accepted: April 24th, 2024

[1] Materials engineer, Universidad Simón Bolívar, Venezuela. MSc in Mechanical Engineering, Universidad Central de Venezuela, Venezuela. Affiliation: Department of Physical Metallurgy, Faculty of Engineering, Universidad Central de Venezuela, Venezuela. E-mail: eudiblanco@gmail.com

[2] Mechanical engineer, Universidad Politécnica Salesiana, Ecuador. PhD in Engineering, Universidad Pontificia Bolivariana, Colombia. Affiliation: New Materials and Transformation Processes Research Group (GiMaT), Mechanical Engineering Faculty, Universidad Politécnica Salesiana, Ecuador. E-mail: jfajardo@ups.edu.ec

[3] Metallurgical engineer, Universidad Central de Venezuela, Venezuela. PhD in Mechanics, University of Sciences and Technologies of Lille, France, and PhD in Engineering Sciences, Universidad Central de Venezuela, Venezuela. Affiliation: Research Group on Characterization, Processing and Protection of Materials, Faculty of Science and Engineering, Universidad Estatal de Milagro, Ecuador. E-mail: ecarrasqueror@unemi.edu.ec

[4] Degree in Chemistry, Universidad Central de Venezuela, Venezuela. PhD in Science, with an emphasis on Chemistry, Universidad Central de Venezuela, Venezuela. Affiliation: Dr. Mitsuo Ogura Center for Electron Microscopy, Faculty of Sciences, Universidad Central de Venezuela, Venezuela. E-mail: caribayurbina@gmail.com

[5] Mechanical engineer, Universidad Politécnica Salesiana, Ecuador. PhD in Industrial Engineering, Universidad San Marcos, Perú. Affiliation: New Materials and Transformation Processes Research Group (GiMaT), Mechanical Engineering Faculty, Universidad Politécnica Salesiana, Ecuador. E-mail: llopez@ups.edu.ec

[6] Mechanical engineer, Universidad Pontificia Bolivariana, Colombia. PhD in Industrial Engineering, Polytechnic University of Madrid, Spain. Affiliation: Research Group on New Materials, School of Engineering, Universidad Pontificia Bolivariana, Colombia. E-mail: luis.cruz@upb.edu.co

Introduction

The tribological properties of composites play an important role in the selection of materials for different purposes. As the composite materials used in industries are exposed to different types of wear (*e.g.*, adhesive or abrasive wear) during their service life, it is very important to consider their tribological performance. Moreover, by considering the tribology of composite materials, we can save a lot of the energy wasted in overcoming the friction between two moving surfaces (Kerni *et al*., 2020). Recent research has focused on studying the friction and wear properties of polymers reinforced with natural fibers. Progress has been made towards improving these properties in composites, in light of the fact that 90% of mechanical part failures are due to tribological loading conditions (Yousif *et al*., 2007). Polymers' wear and friction behavior can be improved or deteriorated by the incorporation of fibers as reinforcement (Bajpai *et al*., 2012).

Polymers are the most commonly used matrices in natural fiber composites due to their light weight. They can be processed at low temperatures. Both thermoplastic and thermoset polymers have been used for matrices with natural fibers. Matrix materials have temperature limitations because most natural fibers are thermally unstable above 200 °C. Thermoplastics (such as polyethylene, polypropylene, polyvinyl chloride, and polystyrene) and thermosets (such as epoxy resin, unsaturated polyester, PF, and vinyl ester) are mainly used in the matrix. Thermoplastics can be softened by applying heat and hardened by cooling. They can therefore be easily recycled (Jariwala and Jain, 2019).

In some applications such as bearings, where one part slides over another, wear is often significant. As low friction is essential, thermoplastics like polypropylene perform well in these applications. These thermoplastics offer a number of additional benefits in addition to wear resistance, such as good corrosion resistance, lower weight, and less noise. Parts made from these thermoplastics also tend to generate less friction and heat, which increases service life and ultimately reduces maintenance costs.

The effect of accelerated thermal aging on the tribological behavior of polypropylene reinforced with bamboo fibers is not sufficiently studied in the literature, so this work is a contribution to the knowledge of the effect of this type of aging on the wear and friction behavior of this biocomposite. Noting the enormous advantages and opportunities associated with natural fibers, in addition to the promising application of polymeric biocomposites in the automotive industry, it is necessary to further investigate the tribological properties of these materials after aging. For this industry, and in many others, long-term stability is important because thermal and oxidative degradation is known to affect the performance of polymer composites.

Methodology

Materials

Isotactic polypropylene (PP) homopolymer was used as polymeric matrix, whose melt flow index (MFI) was 12 g/10 min (at 230 °C/2.16 kg), measured under ISO 1133-1:2011 (2011). The polypropylene matrix was reinforced with randomly oriented bundles of short *Guadua angustifolia* Kunth (GAK) fibers obtained through the steam explosion technique, with a length distribution of 1.0 ± 0.5 mm and a diameter distribution of 0.4 ± 0.2 mm. The onset temperature of degradation was 200 °C. We used maleic anhydride grafted polypropylene (MAPP), with a weight-average molecular weight (Mw) and number-average molecular weight (Mn) of 9100 and 3900, respectively, as the coupling agent between the fiber and the matrix. Molecular weights were determined through the gel permeation chromatography (GPC) method. A maleic anhydride percentage of 8% was used.

Composite processing

PP/Bamboo fiber (PP/FB) composite pellets were prepared using a Dr. Collin E-20 T single-screw extruder, with the following composition: PP with 20 wt% BF (PP/20F), PP with 30 wt% BF (PP/30F), and PP with 40 wt% BF (PP/40F). Then, type 1B 527 ISO standardized specimens (Figure 1) – as per ASTM D638-14 (ASTM International, 2014) – were injected with the different compositions using a Dr. BOY injection molding machine E35. From the specimens obtained by injection, 15 × 15 × 5 mm samples were cut using a Struers Minitom low-speed precision cutting machine with a diamond disc.

Figure 1. Type 1B 527 ISO standardized specimen (ASTM D638-14) made of PP/20F biocomposite, from which the samples for the study were extracted
Source: Authors

Accelerated thermal aging

A group of raw PP and PP/FB samples were subjected to a thermal aging process by continuous heating at 98 °C for 10 days using a BLUE M SW-11TA-1 gravity convection oven (Figure 2). Subsequently, the samples were removed from the oven to cool to room temperature. The temperature selection for this heat treatment was based on its proximity to the continuous-use temperature of homopolymer polypropylene (100 °C).

Figure 2. Gravity convection oven used to perform the accelerated thermal aging test
Source: Authors

Sliding wear tests

The tribological study of PP/FB composites was carried out via sliding wear tests, according to ASTM G99-17 (ASTM International, 2017). These tests were carried out on a standard CSM Instruments tribometer (Figure 3), under the Pin-on-Disk configuration, which consisted of sliding a stationary pin (which acts as a support for the sphere or ball) against the surface of the sample under study coupled to a rotating disk (Figure 4). This equipment includes softwarolled relative humidity of 70 ± 2%. The sliding conditions were as follows: 31 836 cycles, equivalent to a total sliding distance of 600 m; a linear sliding velocity of 15 cm/s; and an applied normal load of 10 N. The static counterparts used were 6 mm diameter spheres of AISI 52100 steel.

Figure 3. Tribometer used for the study of sliding wear
Source: Authors

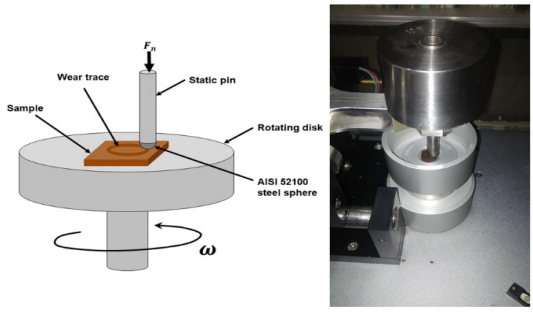

Figure 4. Tribometer used for the study of sliding wear
Source: Authors

For each of the sliding wear tests, the average coefficient of friction values (μ_p) was obtained, and, subsequently, the wear rate (K) was calculated using Equation (1).

$$K = \frac{V_w}{F_n \cdot d} \qquad \left[\text{mm}^3/\text{N}\cdot\text{m}\right] \tag{1}$$

where V_w is the wear volume in [mm^3], F_n is the applied normal load in [N], and d is the total sliding distance in [m]. Equation (2) was used to determine V_w.

$$V_w = \frac{\Delta m}{\rho}\cdot 1000 \quad [\text{mm}^3] \tag{2}$$

where Δm is the mass loss of the specimens in [g] and numerically represents the difference in mass of the specimens before and after the tribology test; ρ is the density of the PP and PP/FB specimens in [g/cm^3], which was obtained by following ASTM D4892-14(2019)e1 (ASTM International, 2019). The values of the densities of the samples are shown in Table 1. The mass difference (Δm) was determined using a Gram digital precision balance, model FR-500.

Table 1. Densities (ρ) of the PP and PP/FB samples

Sample	ρ [g/cm^3]
PP	0.905
PP/20F	0.960
PP/30F	0.990
PP/40F	1.030

Source: Authors

In addition, the friction coefficient achieved by each sample was analyzed and presented in terms of friction fluctuations ($\Delta\mu$), the friction stability coefficient (μ_s), and the coefficient of variability (μ_v). These parameters were calculated through the following formulas (Singh *et al*., 2019):

$$\mu_s = \frac{\mu_p}{\mu_{max}} \tag{3}$$

$$\mu_v = \frac{\Delta\mu}{\mu_p} \tag{4}$$

where μ_p is the average μ recorded for all tests, and $\Delta\mu$ is the difference between the maximum (μ_{max}) and minimum (μ_{min}) values of μ obtained in each test.

Scanning electron microscopy (SEM)

After performing the tribological tests, high-resolution images of the wear traces of all PP and PP/FB samples, with and without aging, were obtained using a scanning electron microscope (FEI, model QUANTA FEG 250) with a secondary electron detector. The surfaces to be visualized were previously metalized by applying a gold (Au) coating using an ion sputter metallizer.

Results and discussion

Effect of fiber content on friction and wear of PP/FB biocomposites

Figure 5 shows the variation of the friction coefficient (μ) with sliding distance for raw PP and PP/FB biocomposites. The friction value increased during the initial phase of wear, which is due to the increase in the contact area between the polymer and the metallic counterpart. Thereafter, it stabilizes and follows a steady state behavior.

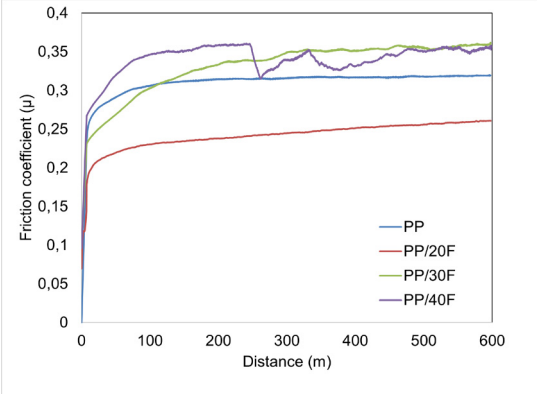

Figure 5. Variation of the friction coefficient (μ) with the sliding distance
Source: Authors

The fluctuations of the friction coefficient (Δμ) are measured as the difference between the highest and lowest μ value reached in each of the tests. This is shown in Figure 6. It can be observed that the fluctuations increase with the increase in bamboo fiber content. Within the group of composite materials, the PP/20F sample showed the lowest fluctuation (0.19).

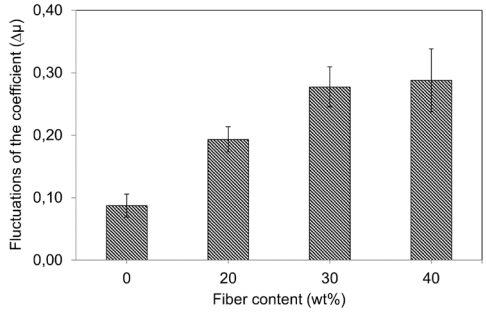

Figure 6. Variation of μ fluctuations (Δμ) with bamboo fiber content
Source: Authors

Moreover, the coefficients of friction stability (μ_s) and variability (μ_v) were calculated for the materials (Figure 7). For a good friction behavior of the material, high μ_s values (close to 1) and low μ_v values (close to 0) are generally needed (Singh *et al.*, 2019). In the tribology tests carried out on the samples, it was found that the μ_s value gradually decreases with the percentage of bamboo fibers, while the μ_v value increases. These results showed that noticeable fluctuations of μ are obtained when PP is reinforced with bamboo fibers, and that these fluctuations increase when the number of fibers in the polymeric matrix is increased. Inadequate fiber distribution or mixing at a higher ratio (40 wt%) may cause structural discontinuities in the composites and thus result in higher friction variability. Meanwhile, at a lower ratio (20 wt%), homogeneity in the mixture could have been achieved, resulting in high friction stability (Singh *et al.*, 2019), as observed in Figure 5.

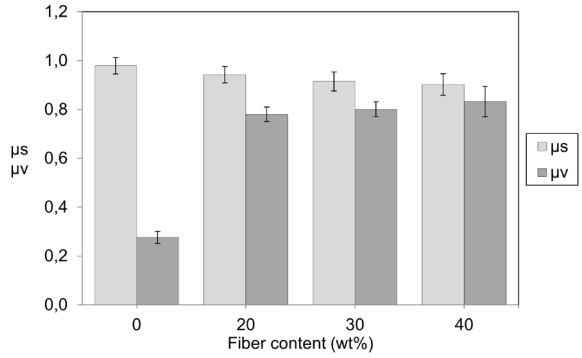

Figure 7. Variation in the coefficients of friction stability (μ_s) and variability (μ_v) with the bamboo fiber content
Source: Authors

The graph in Figure 8 shows the variation of μ with the fiber content of the PP/FB composites, and Table 2 shows the values obtained for this coefficient. PP recorded a decrease of -21.6% of its μ when reinforced with 20 wt% of bamboo fibers. This may be due to the presence of wear particles, commonly called *debris*, *i.e.*, polymer residues that accumulate and plastically deform in the wear trace, creating a soft polymer film that causes a decrease in friction or adheres to its sliding counterpart in a phenomenon called *continuous film transfer* (Nirmal *et al.*, 2012). This film prevents the polymer from coming into direct contact with the metal counterpart material, thus preventing abrasive action and reducing the rate of wear. The thinner and more well distributed the film, the lower the values of the friction and wear coefficients (Mimaroglu *et al.*, 2018). Therefore, the PP/20F composite showed a better performance against friction.

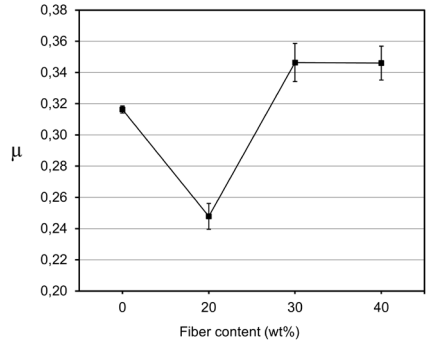

Figure 8. Variation of μ with a fiber content of PP/FB biocomposites
Source: Authors

On the other hand, the μ value of PP shows increases of 9.5 and 9.3% when reinforced with 30 and 40 wt% bamboo fibers, respectively. A higher reinforcement content in turn generates a greater number of fibers exposed during the sliding wear tests. Such fibers tend to detach or fracture and form debris, or a 'third body' between the (metal-polymer) contact surfaces (Nirmal *et al*., 2012; Narish *et al*., 2011). This can cause high relative motion shear strength during sliding wear testing, thereby contributing to a much higher friction coefficient value (Nirmal *et al*., 2012).

Although the plastic component of the biocomposite produces the soft layer of polymer that causes the friction coefficient to decrease, the presence of the fiber is also essential to increasing wear resistance. An amount of fiber greater than 20 wt% causes an increase in the friction coefficient of the biocomposite but could provide the PP with better wear resistance.

Table 2. Coefficient of friction (μ) and wear factor (K) obtained for raw PP and PP/FB biocomposites

Sample	μ	K [×10^{-4} mm^3/N m]
PP	0.3163 ± 0.0023	1.3808 ± 0.0836
PP/20F	0.2478 ± 0.0083	1.0416 ± 0.0220
PP/30F	0.3464 ± 0.0122	1.1784 ± 0.0656
PP/40F	0.3460 ± 0.0108	1.2944 ± 0.0263

Source: Authors

Figure 9 shows the variation of the wear rate (K) with the number of fibers in the composites, whose values are shown in Table 2. In the results obtained for this important tribological parameter, it can be seen that the wear rate of PP decreases with the presence of fibers, with the PP/20F composite showing the lowest K value, representing a decrease of -24.6% in the K value obtained for pure PP. According to the studies carried out by Blanco *et al*. (2020), the stiffness of PP increases with the content of bamboo fiber, given the reinforcing effect (decreasing tenacity) that this fiber achieves in PP. Materials with high stiffness have a better wear behavior, since the contact area between the metal and the polymer is reduced and the shear strength increases (Sınmazçelik and Yılmaz, 2007). Therefore, PP/FB composites exhibited a low wear rate compared to PP without fibers. Specifically, the PP/20F composite achieved a higher wear resistance, which could be due to the better bonding between matrix and fiber (Mimaroglu *et al*., 2018) that occurs during the manufacture of the composite, since at low reinforcement concentrations (20 wt%), a greater contact area between both components or a greater impregnation of the fibers is achieved and, consequently, a better reinforcement, which translates into a higher wear resistance (Sınmazçelik and Yılmaz, 2007). On the other hand, increasing the fiber content to 30 and 40 wt% also resulted – although to a lesser extent – in a decrease in the wear rate of PP (-14.4 and -65.%, respectively). Therefore, fiber reinforcement reduces the wear rate of the composites (Sınmazçelik and Yılmaz, 2007), with PP/20F exhibiting the best performance against wear.

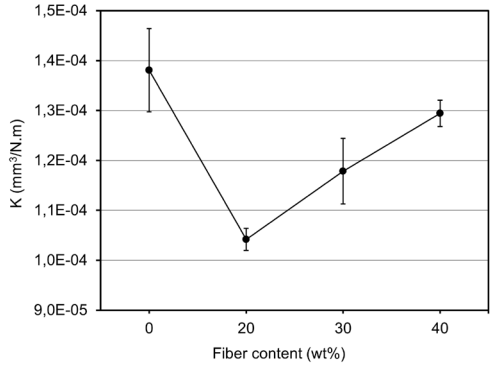

Figure 9. Variation of wear rate (K) with a fiber content of PP/FB biocomposites
Source: Authors

In the group of PP/FB biocomposites, there was a progressive increase in K as the amount of fiber increased from 20 to 40 wt%, with the PP/40F composite producing the highest wear rate within the group, which represented an increase of 24% over that obtained by the PP/20F composite. This means that the amount of wear in the PP/FB samples increased with the fiber content. Such behavior may be due to a loss of reinforcement of the composites, caused by the detachment of the fibers from the polymeric matrix during tribological tests. The increase in the weight percentage of fibers in the polymer matrix produces a greater detachment of the fibers due to a localized temperature increase at the contact surface between the metal and the sample (Sınmazçelik and Yılmaz, 2007). In general, the low tribological performance of polymers may be related to their viscoelasticity and thermal properties. Sliding contact between the specimen and the metal counterface results in heat generation at the asperities, which in turn increases the temperature at the interface. The formation of thermal gradients due to non-uniform temperature distributions creates thermal stresses in the specimen during sliding. These stresses weaken the natural adhesion of the fiber and matrix, causing the fibers to loosen and become easily sheared as a result of repeated axial thrust (Yallew *et al*., 2014). This loosening of the fibers is usually greater the higher the fiber content of the composite (40 wt% in this case). Furthermore, the increase in temperature, generated by the thermomechanical loading, softens the surface of the polymer, which entails decreased hardness. Likewise, there is a dramatic loss in shear strength and, therefore, the penetration resistance of the metallic counterpart decreases. Consequently, higher wear volumes are produced (Sınmazçelik and Yılmaz, 2007; Nirmal *et al*., 2012).

Effect of thermal aging on friction and wear of PP/FB biocomposites

Figure 10 shows a comparison between the friction curves of thermally aged and non-thermally aged PP without fibers and PP/FB samples. The results show that the aged samples

produced higher friction coefficients than the unaged ones – such behavior will be explained later. The average μ values obtained for the aged samples are shown in Table 3.

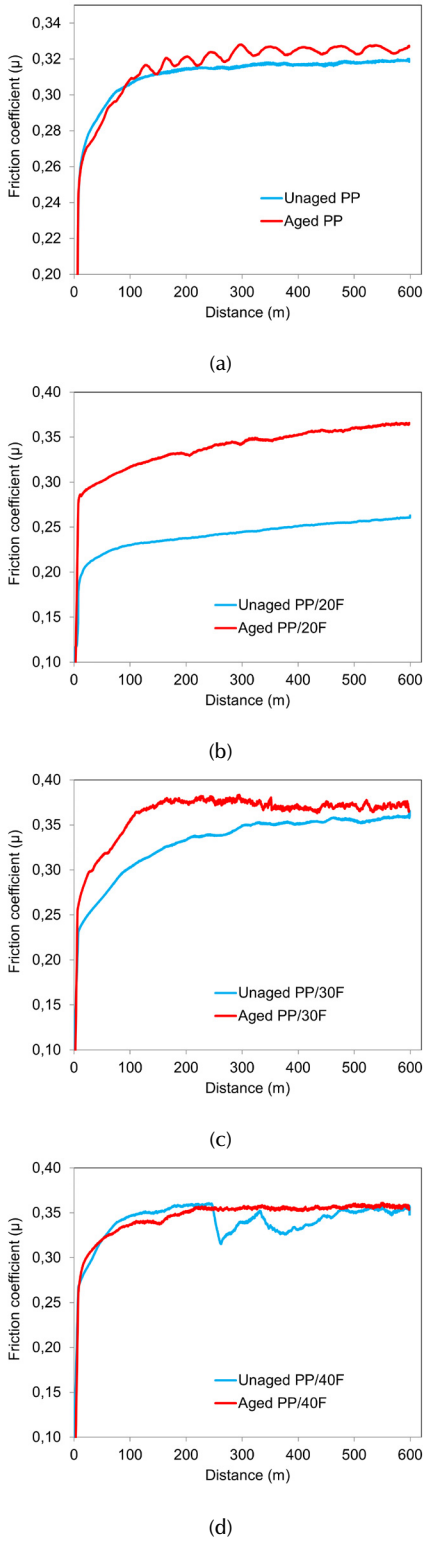

Figure 10. Comparison of the coefficient of friction (μ) *vs.* the sliding distance curves for aged and unaged samples of a) PP, b) PP/20F, c) PP/30F, and d) PP/40F
Source: Authors

Table 3. Coefficient of friction (μ) and wear factor (K) obtained for the aged materials

Sample	μ	K [×10^{-4} mm^3/N m]
PP	0.3230 ± 0.0039	2.8589 ± 0.0362
PP/20F	0.3482 ± 0.0124	1.1285 ± 0.1228
PP/30F	0.3726 ± 0.0042	1.2630 ± 0.0738
PP/40F	0.3538 ± 0.0052	1.3751 ± 0.0586

Source: Authors

It is important to note that the comparative analyses presented below are based on a comparison of the friction parameters (μ_v, μ_s, and μ) and the wear rate (K) obtained for the aged and non-aged samples. All this, while keeping the fiber content fixed.

Figure 11 shows a comparative plot of the friction coefficient of variability (μ_v) of the aged and unaged samples. The aged PP/40F composite exhibited a greater decrease in μ_v (-65.8%) than the unaged sample, *i.e.*, for the PP/40F composite, aging significantly improved the stability of the friction coefficient values, which is evident in Figure 10d.

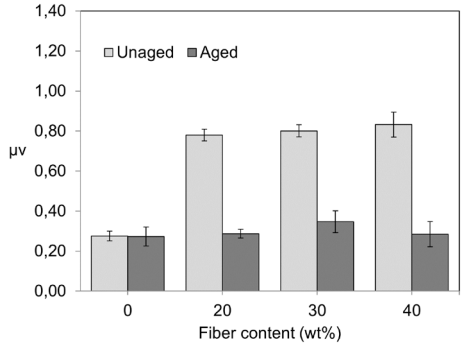

Figure 11. Comparison of the coefficient of friction variability (μ_v) of aged and unaged PP and PP/FB samples
Source: Authors

Figure 12 shows a comparison of the coefficient of friction stability (μ_s) obtained for the aged and unaged PP and PP/FB samples. The highest stability in μ_s values during sliding wear tests occurred with the aged PP/30F and PP/40F composites. This improvement in the friction stability of the composites with a higher percentage of fibers could be due to the increase in the stiffness obtained when they are previously subjected to isothermal heating for some time (Blanco *et al.*, 2020; Blanco-Sánchez *et al.*, 2022).

Figure 13 depicts a graph comparing the value of μ obtained for the aged and unaged samples. This graph confirms what was observed in Figure 10: this parameter increased as a consequence of aging in all the samples. This increase was more noticeable in the PP/20F composite, and less marked in raw PP and PP/40F. After thermal aging, the coefficient of friction of the PP/20F composite increased by 40.5%, while, for the raw PP and the PP/30F and PP/40F composites, the

increase was 2.1, 7.5, and 2.2%, respectively. The aged PP/30F composite showed the highest μ value (0.37).

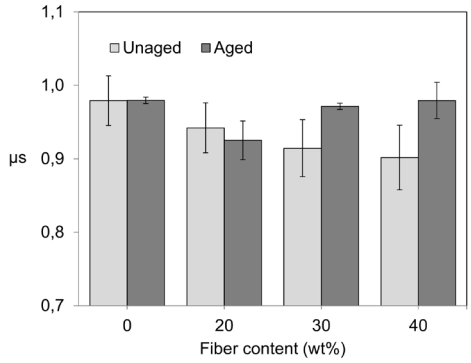

Figure 12. Comparison of the coefficient of friction stability (μ_s) of aged and unaged PP and PP/FB samples
Source: Authors

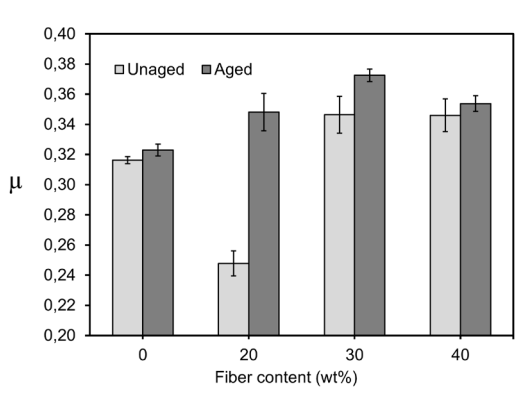

Figure 13. Effect of thermal aging on the coefficient of friction (μ) of raw PP and PP/FB biocomposites
Source: Authors

The increase in the friction parameter of the samples, due to thermal aging, could be due to the secondary crystallization process of PP (annealing) that occurs during heating, which can lead to an increase in the degree of crystallinity or the size of the pre-existing polymer crystals. This makes these materials stiffer and represents a significant decrease in toughness, increasing shear strength especially when there is a low amount of fiber in the matrix (PP/20F) (Inácio *et al.*, 2018; Sınmazçelik and Yılmaz, 2007; Blanco *et al.*, 2020; Blanco-Sánchez *et al.*, 2022, Law *et al.*, 2008), and, as a consequence, an increase in the coefficient of friction of the material occurs. The increase of μ in the composites with a higher bamboo fiber content (PP/30F and PP/40F) could be mostly due to the presence of a higher number of exposed fibers in the surface layer during sliding wear tests, which are easily detached from the matrix given the possible weakening and/or rupture of the polymer/compatibilizer bonds due to aging (Inácio *et al.*, 2018). These shed fibers tend to form material debris in the space between the metal and the polymer, thus causing increased friction between the two surfaces (Nirmal *et al.*, 2012).

Figure 14 compares the K values obtained for the aged and non-thermally aged samples. In this graph, it can be observed that the aged samples reached a low wear resistance compared to the unaged ones. This behavior could be attributed to an embrittlement of the samples, a product of the increase in the crystallinity of the polymer during thermal aging (Inácio *et al.*, 2018; Sınmazçelik and Yılmaz, 2007). Consequently, the material tends to fracture at very low deformations (Blanco *et al.*, 2020) during the sliding wear process. Furthermore, as noted above, thermal aging also weakens the bonds between the polymer and the coupling agent (MAPP). Thus, a loss of the reinforcing effect of the bamboo fiber in the PP matrix takes place, making the aged composites less wear-resistant than the unaged ones.

The loss of wear resistance due to aging was more noticeable in the unreinforced PP, which can be attributed to the high brittleness that could have been reached by the PP without fibers due to the increase in crystallinity during thermal aging (Sınmazçelik and Yılmaz, 2007; Blanco *et al.*, 2020; Law *et al.*, 2008), wherein the polymer chains have greater freedom of movement, since there are no bamboo fibers present in their volume, to increase the size of the pre-existing crystals or to form new crystals within the amorphous regions (Blanco-Sánchez *et al.*, 2022). On the other hand, the wear rate of aged and unaged PP/20F was the lowest compared to that of the rest of the composites (Figure 14).

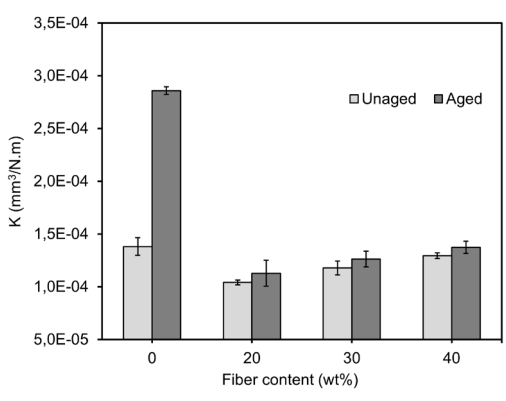

Figure 14. Effect of thermal aging on the wear rate (K) of raw PP and PP/FB biocomposites
Source: Authors

SEM analysis

The tribological behavior of the PP/FB composites can also be explained by analyzing the SEM images of their wear surfaces. Figure 15 presents the micrographs of the wear traces belonging to the pure PP samples and the PP/FB composites without thermal aging. Figure 15a corresponds to the wear surface of the PP without fibers, showing the formation of a film of plastically deformed polymeric material, as well as the presence of micro-cracks, delamination, and polymer residues (debris). In Figures 15c and 15d, corresponding to the wear traces of PP/30F and PP/40F, respectively, a great deterioration of the surface can be seen, which evinces the low wear resistance of

both composites. In these Figures, the four severe wear mechanisms that normally occur in polymeric biocomposites are observed: (i) matrix wear (debris, plastic deformation, plowing, shearing, and cracking); (ii) fiber wear by sliding; (iii) fiber pullout or fracture; and (iv) loss of fiber-matrix interaction (Sınmazçelik and Yılmaz, 2007). Figure 15b shows the polymer film on the wear surface of PP/20F, with the presence of finely divided and loose polymer particles at the edge of the footprint, as produced by matrix wear. The wear surface is relatively smooth, indicating that the wear damage was slight (Bhushan, 2013). However, it was noted that the plastically deformed polymer film on the tread showed uniformly distributed 'prow' marks (Martínez *et al*., 2010) and did not show cracking or appreciable fiber detachment, which constitutes evidence of PP/20F's better wear performance compared to the rest of the composites, in agreement with the results shown in Figure 9.

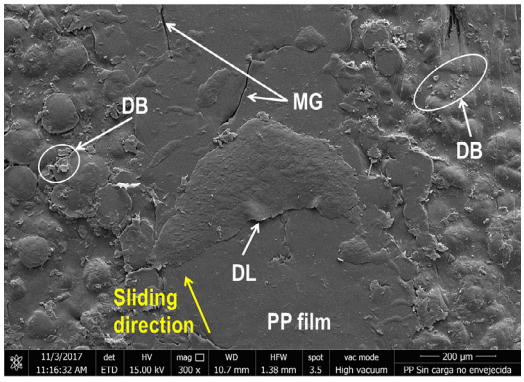

(a)

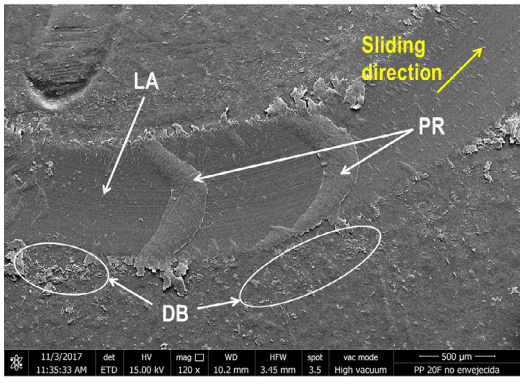

(b)

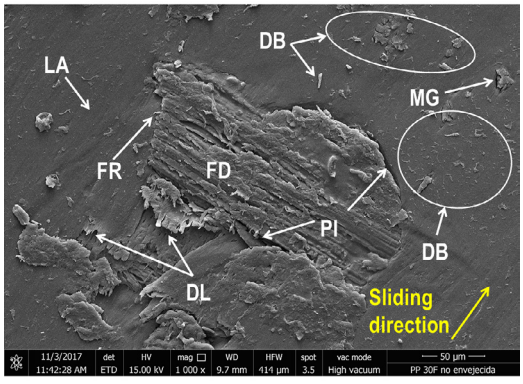

(c)

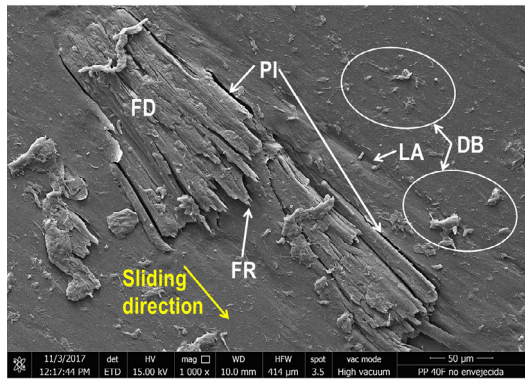

(d)

Figure 15. Worn and unaged surfaces of: a) PP without fibers, b) PP/20F, c) PP/30F, and d) PP/40F. Abbreviations: DB: debris; DL: delamination; FD: worn fiber bundle; FR: fiber fracture; MG: microcrack; LA: plow lines; PI: fiber-matrix debonding; PR: prow.
Source: Authors

Further micrographs of the wear traces of the PP/30F and PP/40F composites are shown in Figures 16a and 16b, respectively. In both composites, polymer debris was observed, and many remains of detached or fractured fibers embedded in plastically deformed polymer debris and adhered to the wear surface. Such remains of fibers possibly formed a 'third body' between the contact surfaces (metal-polymer), producing a high shear strength during the sliding wear test, which produced higher friction between the tribological pair and a higher wear of the composites. This behavior corresponds to the results of the friction coefficient and wear rate, as shown in the graphs of Figures 8 and 9, respectively, wherein the PP/30F and PP/40F composites reached the highest values of μ and K compared to the PP/20F composite.

Thin wear particles (debris) in the form of plaque or flakes were observed in Figure 17a, which are commonly found during the sliding of dry and lubricated interfaces. These particles are produced as a result of plowing (abrasive wear), which can also be seen in Figure 17a, due to the rubbing of the asperities of the metal part against the polymer surface. After the surface has been plowed several times, material removal can occur by a low-cycle fatigue mechanism. When plowing occurs, ridges form along the sides of the plowed grooves. These ridges flatten and eventually fracture after repeated loading and unloading cycles. The plowing process also causes plastic deformation of the subsoil and may contribute to the nucleation of surface and subsurface cracks. Additional loading and unloading (high-stress, low-cycle fatigue) causes these cracks, voids, and pre-existing cracks to propagate (subsurface cracks propagate parallel to the surface to some depth) and coalesce with neighboring cracks that eventually shear at the surface and result in thin wear platelets (Bhushan, 2013; Martínez *et al*., 2010).

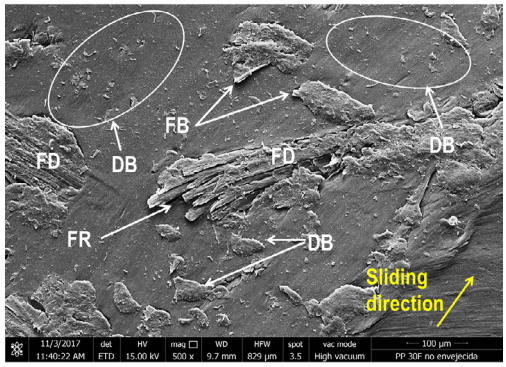

(a)

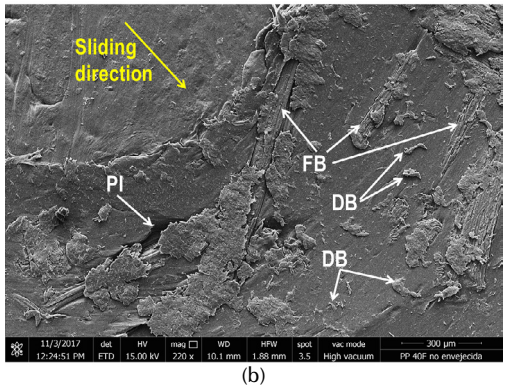

(b)

Figure 16. Worn and unaged surfaces of a) PP/30F and b) PP/40F. Abbreviations: DB: debris; FB: detached fibers; FD: fiber bundle worn; FR: fiber fracture; PI: fiber-matrix unbinding.
Source: Authors

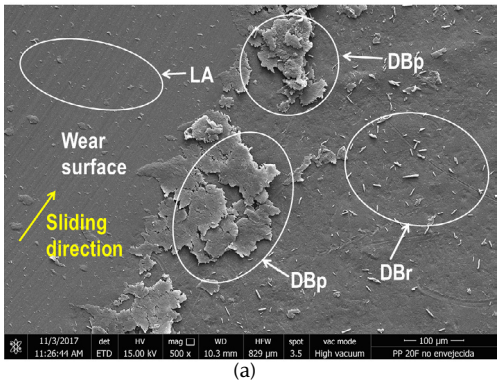

(a)

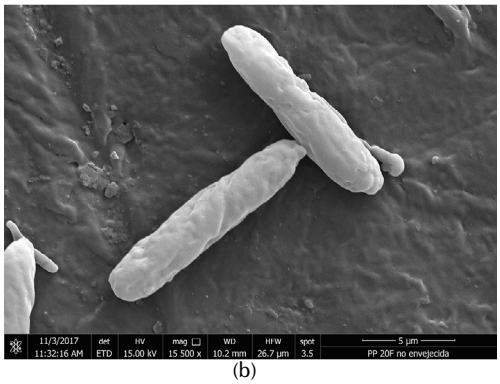

(b)

Figure 17. Worn surface of unaged PP/20F with the presence of wear debris a) in the form of plates or flakes and b) in the form of rollers. Abbreviations: DBp: plate or flake debris; DBr: roller debris; LA: plow lines.
Source: Authors

A characteristic of fatigue wear is material damage under the repetitive action of compressive, tensile, and shear deformations during the cyclic loading caused by the interaction between the metallic counterpart and the rough surface of the polymer during sliding, leading to the generation and development of cracks, which may be favored by the presence of defects. Some authors modify the term *fatigue wear* to *frictional wear* if the polymer exhibits a low resistance to tearing, causing the formation of roller-like particles at the sliding interface and the tearing of the laminated fragment (Martínez *et al*., 2010). In Figures 17 and 18a, the roller-like wear particles can be seen, in addition to the tearing of the polymer component in Figure 18b. This corroborates that the fatigue or frictional wear mechanism was also present during the tribology tests of the PP/FB composites.

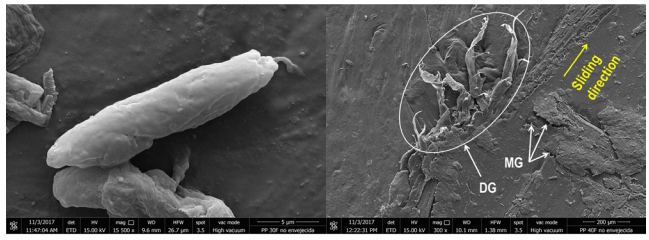

(a) (b)

Figure 18. (a) Polymer wear particles (with roller morphology) observed after wear testing of unaged PP/30F composite; (b) Polymer tearing and cracking observed after wear testing of unaged PP/40F composite. Abbreviations: DG: polymer tearing; MG: microcrack.
Source: Authors

In general terms, according to the results obtained for the μ and K parameters (Figures 13 and 14, respectively), the thermal aging process applied in this work caused an increase in the friction of the materials, as well as a loss of the wear resistance of the PP/FB biocomposites. This loss is more significant in raw PP. The worn surface of the aged fiber-free PP showed signs of delamination, in addition to significant evidence of abrasive wear, as many plow lines were observed (Figure 19a), and a large amount of flake-like polymer particles (Figure 19b). Any wear particles generated on the surface will cause further plowing and increase the frictional force, thereby accelerating the delamination process (Martínez *et al*., 2010). The low temperature at which most polymers melt, as well as their low thermal conductivity, ensures that frictional contact temperatures can easily reach the melting point of the polymer, causing its surface to melt, entailing the formation of a 'prow'. The effect of 'prow' formations over the entire wear trace of the polymer is known as fatigue wave formation (Bartenevev and Lavrentev, 1981), which was also observed, very noticeably, on the wear surface of the aged raw PP (Figures 19b and 19c) and the unaged PP/20F (Figure 15b). These waves are associated with the fatigue mechanism, given the cyclic passage of metal counterbody asperities on the polymer surface, as well as with a melt wear mechanism (da Silva *et al*., 2007). All this evidence on the contact surface demonstrates

the significant loss of wear resistance of the PP without fibers due to thermal aging. Nevertheless, this loss of wear resistance was found to be lower in the PP/FB composites (Figure 14).

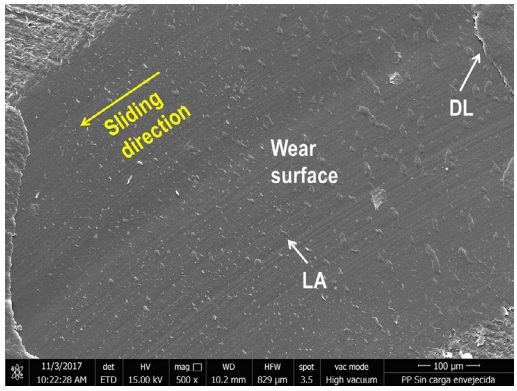

(a)

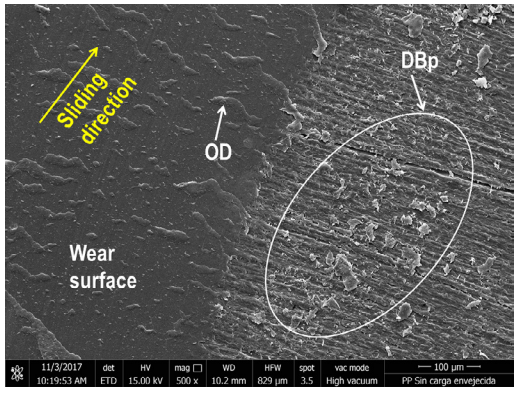

(b)

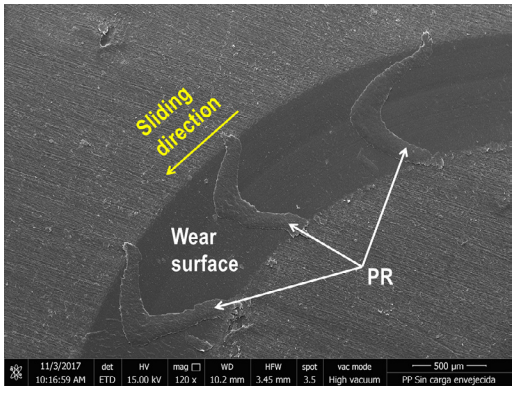

(c)

Figure 19. Worn surfaces of aged PP with the presence of a) plow lines (abrasive wear), b) flake-like polymer debris (adhesive wear), and c) prows. Abbreviations: DL: delamination; DBp: plate or flake debris; LA: plow line; OD: waves; PR: prow.
Source: Authors

The wear mechanism exhibited by the biocomposites (Figure 20) could be related to delamination. This phenomenon occurred due to the stratified nature of the stress state in the Hertzian zone, as a result of the frictional or tangential load that generates a shear stress field on the surface and subsoil. The maximum values of these shear stresses are reached at a certain distance from the surface. Likewise, the stress state generated by the different cyclic loads acting in the contact zone favored the cracks to nucleate below the surface (where shear stresses are maximal) and propagate to the surface. This propagation of cracks and their extension to neighboring cracks and surface shear cause the wear lamellae to delaminate after a large number of asperities pass through each point on the surface of the material (da Silva *et al*., 2007).

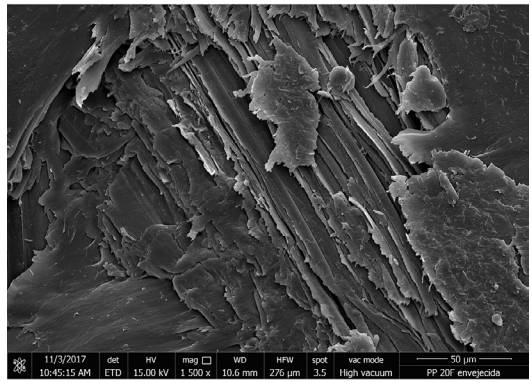

(a)

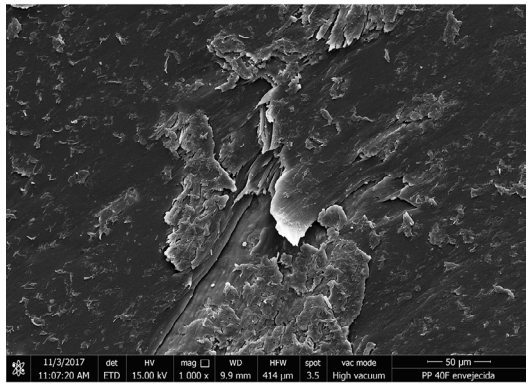

(b)

Figure 20. Wear traces of a) thermally aged PP/20F and b) PP/40F, which show delamination
Source: Authors

In the case of brittle materials with low fracture toughness, wear occurs by brittle fracture. In these cases, the worn zone is characterized by significant cracking (Bhushan, 2013). Figure 21 shows the wear traces of PP/20F and PP/30F composites with the presence of longitudinal and transverse microcracks towards the sliding direction. The transverse microcracks observed on the surface are consistent with a repeated plowing mechanism causing surface fatigue, while the microcracks observed in the wear direction are formed due to micro-cutting produced by the asperities of the metallic counterpart on the polymer surface (Harsha and Tewari, 2003). Polymer tribology studies by authors such as da Silva *et al*. (2007) state that plowing can cause the formation of cracks on the worn surface as a result of the high tensile stresses generated in the contact zone. In addition, the propagation of these cracks results in surface tearing.

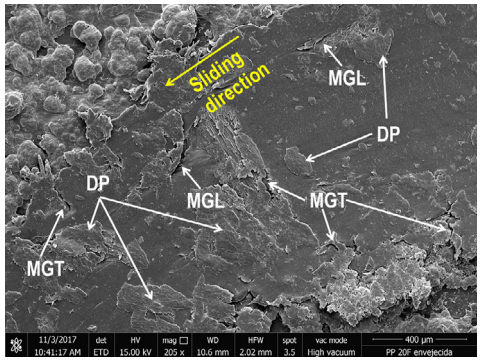

(a)

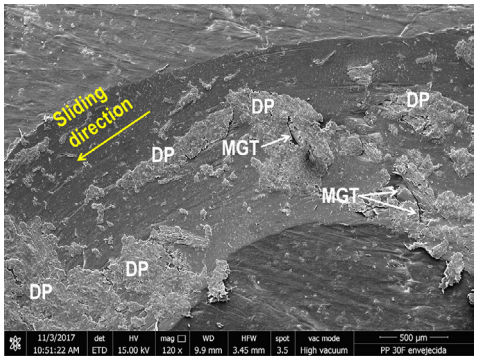

(b)

Figure 21. Wear traces of thermally aged a) PP/20F and b) PP/30F, showing cracking. Abbreviations: PD: plastic deformation; MGL: microcrack longitudinal to the sliding direction; MGT: microcrack transverse to the sliding direction.
Source: Authors

In adhesive wear, the localized cold welding of asperities takes place due to the very strong adhesive forces that occur when two surfaces slide against each other. However, as the yield strength of these cold-welded joints is exceeded, these asperities deform plastically, which typically occurs in a softer material when it slides against a harder surface (Narish *et al*., 2011). Figure 21 shows the abraded surfaces of aged PP/20F and PP/30F biocomposites. These surfaces have attached patches of polymeric material, characterized as *plastic deformation*. This surface characteristic is common in the predominant adhesive wear mechanism in all the sliding wear tests performed in this work. However, these surface defects were mostly observed in the wear trace of the aged PP/30F (Figure 21b), generating higher friction between the tribological pair, which is why that composite reached the highest value of μ (Figure 13).

Another reason why thermal aging caused the biocomposites to have lower wear resistance when compared to the samples without aging was the damage caused to the fiber by the action of an abrasive wear mechanism. Figure 22a presents a micrograph showing the abrasive wear of a bundle of bamboo fibers, characterized by the fracture and tearing of several fibers. In addition, the wear debris appears as fine fibrils cut from the polymeric matrix that adheres to the surface (abrasive wear) (Harsha and Tewari, 2003).

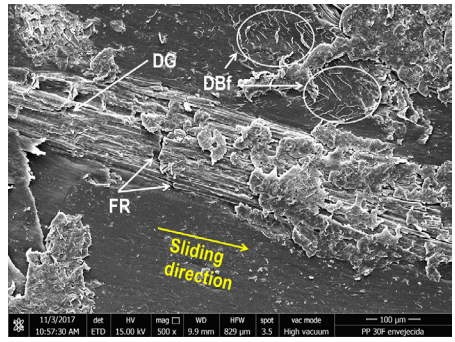

(a)

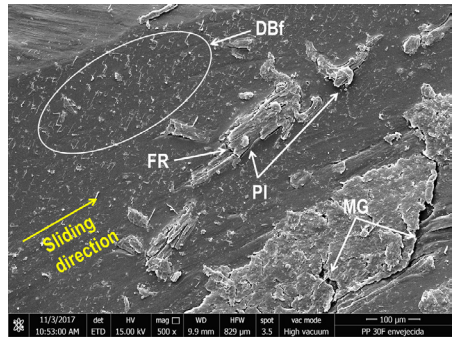

(b)

Figure 22. Wear trace of thermally aged PP/30F showing a) fiber abrasion wear and (b) loss of fiber-matrix interaction. Abbreviations: DG: fiber tearing; DBf: fibril polymer debris; FR: fiber fracture; MG: microcrack; PI: fiber-matrix debonding.
Source: Authors

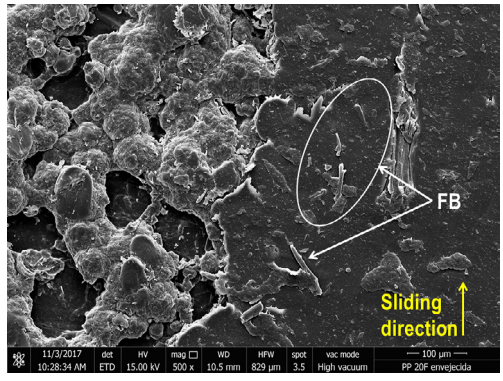

Figure 23. Remnants of bamboo fibers and delamination were observed in the wear trace of thermally aged PP/20F. Abbreviations: FB: detached fiber.
Source: Authors

The prolonged exposure of PP/FB composites to environments with temperatures close to the continuous-use temperature of PP (98 °C) causes a decrease in fiber-matrix interaction, which results in a loss of wear resistance. This decreased interaction is likely attributed to a loss of moisture from the fiber during thermal aging, resulting in micro-embrittlement around the fibers, which reduces the area of the fiber-matrix interface, thus decreasing the shear strength at the interface (Blanco *et al*., 2020). This effect, together with the thermal gradients that occur during sliding wear, given the

non-uniform temperature distribution that creates thermal stresses on the sliding surface, weakens the fiber-matrix adhesion (Figure 22b), which causes bamboo fibers to loosen and become easily sheared as a result of repeated axial thrust during sliding (Yallew *et al*., 2014). This could be the cause for the loosening and fracture of the fibers in the matrix during sliding wear tests, which was also observed in the wear of the thermally aged PP/20F composite (Figure 23) and could have been the reason why this composite exhibited a remarkable increase in its friction coefficient in comparison with the unaged sample (Figure 13).

Conclusions

PP reinforced with 20 wt% of bamboo fibers showed better friction and wear performance, as this percentage of fibers enabled a greater reduction in the coefficient of friction and wear rate of PP (-21.6 and -24.6%, respectively). After thermal aging, the friction coefficient of the PP/20F composite increased by 40.5%, while, for raw PP, PP/30F, and PP/40F, the increase was 2.1, 7.5, and 2.2%, respectively. Likewise, aging caused a loss in the wear resistance of PP and PP/FB composites. This effect was highly noticeable in PP without fibers and less marked in the biocomposites. Greater effectiveness was achieved when the bamboo fiber content was 20 wt%. The use of SEM made it possible to identify the worn surfaces of the raw PP and PP/FB biocomposites. After the tests, some of the wear mechanisms were evidenced, such as prow formation, plowing, cutting, tearing, melting, wave formation, and adhesion. Adhesive, abrasive, and fatigue wear were the dominant ones in the tribology tests of these materials.

CRedit author statement

Eudi Blanco: conceptualization, investigation, methodology, resources, data curation, formal analysis, validation, writing (original draft), visualization, and writing (review and editing). **Jorge Fajardo and Caribay Urbina**: methodology, validation, writing (review and editing), and resources. **Edwuin Carrasquero, Luis López, and Luis Cruz:** validation and writing (review and editing). All authors contributed to the writing of the manuscript and approved its final version for publication.

References

ASTM International (2014). *Standard test method for tensile properties of plastics* (*ASTM D638-14*). ASTM. https://doi.org/10.1520/D0638-14

ASTM International (2017). *Standard test method for wear testing with a pin-on-disk apparatus* (*ASTM G99-17*). ASTM. https://doi.org/10.1520/G0099-17

ASTM International (2019). *Standard test method for density of solid pitch* (*helium pycnometer method*) (*ASTM D4892-14*(*2019*)*e1*). ASTM. https://doi.org/10.1520/D4892-14R19E01

Bajpai, P. K., Singh, I., and Madaan, J. (2012). Frictional and adhesive wear performance of natural fibre reinforced polypropylene composites. *Journal of Engineering Tribology, 227*(4), 385-392. https://doi.org/10.1177/1350650112461868

Bhushan, B. (2013). *Principles and applications of tribology*. John Wiley & Sons Ltd.

Blanco, E., Fajardo, J., Carrasquero, E., Urbina, C., and León, J. B. (2020). Estudio de las propiedades a tensión de un material biocompuesto reforzado con haces de fibras cortas de bambú. *Revista UIS Ingenierías, 19*(3), 163-176. https://doi.org/10.18273/revuin.v19n3-2020016

Blanco-Sánchez, E., Madera-Mujica, A., Pérez-Castillo, M., Fajardo-Seminario, J., Carrasquero-Rodríguez, E., López-López, L., and Cruz-Riaño, L. (2022). Influencia del contenido de fibra y del recocido sobre las propiedades térmicas de un material biocompuesto reforzado con fibras de bambú. *Revista UIS Ingenierías, 21*(2), 39-52. https://doi.org/10.18273/revuin.v21n2-2022004

Bartenevev, G. M., and Lavrentev, V. V. (1981). *Friction and wear of polymers*. Elsevier Scientific Publishing Company.

da Silva, R. L. C., da Silva, C. H., Medeiros, J. T. N. (2007). Is there delamination wear in polyurethane? *Wear, 263*, 974-983. https://doi.org/10.1016/j.wear.2007.01.082

Harsha, A. P., and Tewari, U. S. (2003). Two-body and three-body abrasive wear behaviour of polyaryletherketone composites. *Polymer Testing, 22*(4), 403-418. https://doi.org/10.1016/S0142-9418(02)00121-6

Inácio, A. L. N, Nonato, R. C., and Bonse, B. C. (2018). Mechanical and thermal behavior of aged composites of recycled PP/EPDM/talc reinforced with bamboo fiber. *Polymer Testing, 72*, 357-363. https://doi.org/10.1016/j.polymertesting.2018.10.035

International Organization for Standardization (ISO) (2011). *Determination of the melt mass-flow rate* (*MFR*) *and melt volume-flow rate* (*MVR*) *of thermoplastics - Part 1: Standard method* (*ISO 1133-1:2011*). ISO.

Jariwala, H., and Jain, P. (2019). A review on mechanical behavior of natural fiber reinforced polymer composites and its applications. *Journal of Reinforced Plastics and Composites, 38*(10), 441-453. https://doi.org/10.1177/0731684419828524

Kerni, L., Singh, S., Patnaik, A., and Kumar, N. (2020). A review on natural fiber reinforced composites. *Materials Today: Proceedings, 28*(3), 1616-1621. https://doi.org/10.1016/j.matpr.2020.04.851

Law, A., Simon, L., and Lee-Sullivan, P. (2008). Effects of thermal aging on isotactic polypropylene crystallinity. *Polymer Engineering and Science, 48*, 627-633. https://doi.org/10.1002/pen.20987

Martínez, F. J., Canales, M., Bielsa, J. M., and Jiménez, M. A. (2010). Relationship between wear rate and mechanical fatigue in sliding TPU–metal contacts. *Wear, 268*, 388-398. https://doi.org/10.1016/j.wear.2009.08.026

Mimaroglu, A., Unal, H., and Yetgin, S. H. (2018). Tribological properties of nanoclay reinforced polyamide-6/polypropylene blend. *Macromolecular Symposia, 379*, 1700022. https://doi.org/10.1002/masy.201700022

Narish, S., Yousif, B. F., and Rilling, D. (2011). Adhesive wear of thermoplastic composite based on kenaf fibres. *Proceedings of the Institution of Mechanical Engineers, Part J: Journal of Engineering Tribology 225*(2), 101-109. https://doi.org/10.1177/2041305X10394053

Nirmal, U., Hashim, J., and Low, K. O. (2012). Adhesive wear and frictional performance of bamboo fibres reinforced epoxy composite. *Tribology International, 47*, 122-133. https://doi.org/10.1016/j.triboint.2011.10.012

Singh, T., Kumar, N., Ashok Raj, J., Grewal, J. S., Patnaik, A., and Fekete, G. (2019). Natural fiber reinforced non-asbestos brake friction composites: influence of ramie fiber on physico-mechanical and tribological properties. *Materials Research Express, 6*, 115701. https://doi.org/10.1088/2053-1591/ab45a4

Sınmazçelik, T., and Yılmaz, T. (2007). Thermal aging effects on mechanical and tribological performance of PEEK and short fiber reinforced PEEK composites. *Materials and Design, 28*(2), 641-648. https://doi.org/10.1016/j.matdes.2005.07.007

Yallew, T. B., Kumar, P., and Singh, I. (2014). Sliding wear properties of jute fabric reinforced polypropylene composites. *Procedia Engineering 97*, 402-411. https://doi.org/10.1016/j.proeng.2014.12.264

Yousif, B. F., and El-Tayeb, N. S. M.; (2007). Tribological evaluations of polyester composites considering three orientations of CSM glass fibres using BOR machine. *Applied Composite Materials, 14*(2), 105-116. https://doi.org/10.1007/s10443-007-9034-2